CONTROL TEMPERATURE FLUCTUATIONS IN TWO-PHASE CuO-WATER NANOFLUID BY TRANSFIGURATION OF THE ENCLOSURES

by

***Hadi Pourziaei ARABAN*[a], *Javad ALINEJAD*[a*], *and Davood Domiri GANJI*[b]**

[a] Department of Mechanical Engineering, Sari Branch, Islamic Azad University, Sari, Iran
[b] Department of Mechanical Engineering, Babol Noshirvani University of Technology, Babol, Iran

Original scientific paper
https://doi.org/10.2298/TSCI200524334P

The innovation of this paper is to simulate two-phase nanofluid natural convection inside the transformable enclosure to control the heat transfer rate under different heat flux. Heat transfer of a two-phase CuO-water nanofluid in an enclosure under different heat flux has many industrial applications including energy storage systems, thermal control of electronic devices and cooling of radioactive waste containers. The Lattice Boltzmann method based on the D2Q9 method has been utilized for modeling velocity and temperature fields. Streamlines, isotherms and nanoparticle volume fraction, have been investigated for control the heat transfer rate for several cases. The purpose of this feasibility study is to achieve uniform temperature profiles and T_{max} < 50 °C under different heat flux. Natural convection heat transfer in the rectangular and parallelogram enclosures with positive and negative angular adiabatic walls were simulated. The average wall temperature under heat flux boundary condition has been studied to predict optimal levels of effective factors to control the maximum wall temperature. The results illustrated parallelogram enclosures with positive angle of Case 1 and Cases 3 and 4 with rectangular enclosures were best cases for considering physical conditions. Average of temperature for these cases were 37.9, 29.7, and 38.2 °C, respectively.

Key words: *enclosure transfiguration, heat transfer controlling, heat flux, lattice Boltzmann method, natural convection, two-phase nanofluid*

Introduction

Heat transfer of a two-phase CuO-water nanofluid in an enclosure under different heat flux has many industrial applications including energy storage systems, thermal control of electronic devices and cooling of radioactive waste containers. In these applications, control the heat transfer rate of a two-phase nanofluid under different heat flux by transfiguration of the enclosure have been investigated. So it motivated the researchers to improve their accuracy by different ways, such as experimentally, numerically or analytically.

Not only control the heat transfer rate in an enclosure have been improved the heat transfer mechanism, also using a two-phase nanofluid can be assisted the heat transfer in industries which both of these considered in this literature review. The mentioned industrial applications of the hybrid heat transfer [1]. In an attempt to solve many problems, particularly in fluid mechanics, the lattice Boltzmann method (LBM) [2] has been evolving over the last two dec-

* Corresponding author, e-mail: Alinejad_javad@yahoo.com, Alinejad_javad@iausari.ac.ir

ades. Physics of microscopic processes are taken into account by simplifying kinetic models in LBM. Fluid-flows are then anticipated through the evolution of one-particle phase space distribution functions on associated macroscopic average properties. The LBM simulations, based on the gas kinetic theorem, are based on two simple steps: particle distribution *collision* on lattice nodes and stream *propagation* from one node to all neighbors along the lattice directions [3]. Once streaming is done new distribution components of lattice nodes are calculated, from which we obtain the updated macroscopic properties. This method of calculating macroscopic values essentially differs from what is done in other traditional CFD methods [4]. Algorithm simplicity, fully parallel computation and easy implementation of complex boundary conditions are among the numerous superiorities of LBM [5]. The lattice Bhatnagar-Gross-Krook model which is the most popular LBM is known for its remarkable abilities to solve complex fluid-flow problems [6] such as natural convection flow, multiphase fluids and suspensions in fluids. Moreover, it is shown a strong potential in simulating non-linear mathematical-physical equations [7]. It should be noted that these models always deal with stability issues and therefore in the last few years, several researches have been done to solve this problem [8] such as two-relaxation time (TRT) and multi-relaxation-time (MRT) models. Similar to other problems, stability issues exist for natural convection problems when the Rayleigh number is increased excessively. Two different forms of double MRT thermal LBM have been utilized by researchers, namely Alinejad *et al.* [9, 10], to improve the numerical stability. Significantly improved the numerical stability of the thermal LBM. Based on the proposed model by Alinejad *et al.* [11], a simplified 3-D thermal LBM was presented by Fallah *et al.* [12], in which, the compression work and viscous heat dissipation were neglected for incompressible flows. Peiravi *et al.* [13], successfully used the 3-D thermal LBM to simulate different heat transfer problems. Peiravi *et al.* [14, 15] examined the hybrid heat transfer of an unstable fluid in a 2-D channel. Recently Liang *et al.* [16] studied 3-D model of multi-droplet impact on a liquid/vapor two-phase heat transfer on liquid film. Boubaker *et al.* [17] examined an experimental study of effect of self-rewetting fluids on the liquid/vapor phase change in a porous media. Park *et al.* [18] investigated the thermal performance of a heat transfer augmentation in two-phase flow heat exchanger using porous micro-structures and a hydrophobic coating. Burk *et al.* [19] studied computational examination of two-phase micro-channel array with hybrid heat spreading. Zhang *et al.* [20] experimentally investigated on single-phase and two-phase convection flow boiling heat transfer in an inclined rod bundle. Liu *et al.* [21] investigated quantify the uncertainty of multiphase CFD simulations of two-phase flow and boiling heat transfer through a data-driven modular Bayesian approach. Jiang *et al.* [22] studied fluid-flow and heat transfer characteristics of mist/steam two-phase flow in the *U*-shaped cooling passage. Song *et al.* [23] experimentally investigated condensation heat transfer performance on two-phase R14 flow patterns in a horizontal smooth tube. Lee *et al.* [24] experimentally and computationally examined on two-phase flow and heat transfer of highly subcooled nucleate flow boiling in a rectangular channel having two opposite heating walls. Zhang *et al.* [25] experimentally investigated two-phase flow and heat transfer in a self-developed MRI compatible LN2 cryoprobe based cryosurgery system. Moezzi *et al.* [26] numerically investigated hysteretic heat transfer study of liquid-liquid two-phase flow on a T-junction containing water-oil flow in cooling processes of micro-channel. Alinejad *et al.* [40] numerically investigated droplet impact over the qubical sylanders with dynamic contact angeles.

In the present study, the heat transfer of a two-phase nanofluid under different heat flux is modeled to enhance the heat transfer rate by transfiguration of the enclosure. The LBM is used by FORTRAN software code to investigate controlling the heat transfer rate of a two-phase nanofluid under different heat flux by transfiguration of the enclosure. Then the flow and heat transfer characteristics are investigated for a two-phase nanofluid. Finally, in order to study more precisely, control the heat transfer rate under different heat flux by transfiguration of the enclosure have been investigated. In fact, the change in the amount of these parameters have been affected on the Streamline, isotherm, nanoparticle volume fraction, velocity and temperature fields.

Problem definition

The heat transfer rate of a two-phase CuO-water nanofluid under different heat flux in a cubical enclosure is presented. The heat transfer characteristics are controlled by transfiguration of the enclosure. The boundary conditions for the mentioned problem are shown in fig. 1. This figure shows a cubical enclosure that even in six cases of different heat flux but in all of cases, total absolute value of heat flux is as the same and equals q''. The dimensions of cubical enclosure are $L \times L$.

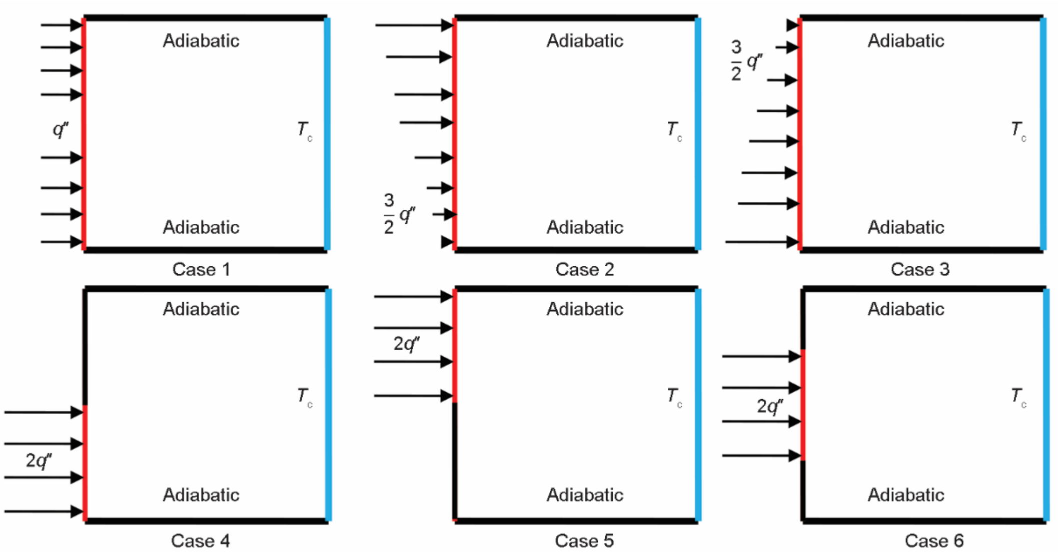

Figure 1. Schematic diagrams of physical models

The flow is considered incompressible and fluid properties are assumed constant except the density whose varying with the temperature. Hydrodynamic boundary conditions for two-phase nanofluid-flow in enclosers are:

$$\begin{cases} u = 0 \\ v = 0 \end{cases} \text{at} \begin{cases} x = 0 \\ x = L \end{cases} \text{and} \begin{cases} y = 0 \\ y = L \end{cases} \tag{1}$$

Simulation methodology

Lattice Boltzmann method

The lattice kinetic theory and especially the LBM have been developed as significantly successful alternative numerical approaches for the solution of a wide class of problems [28]. The LBM is derived from lattice gas methods and can be regarded as a first order

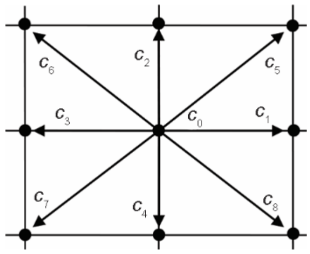

Figure 2. The 2-D vectors for nine-velocity and temperature lattice

explicit discretization of the Boltzmann equation in phase space [29-33]. The LBM is a powerful numerical technique, based on kinetic theory, for simulating fluid-flow and heat transfer [34, 35], and has many advantages in comparison with conventional CFD methods mentioned previously. In contrast with the classical macroscopic Navier-Stokes (NS) approach, the LBM uses a mesoscopic simulation model to simulate fluid-flow [36, 37]. In the LBM, integral distribution functions over boundaries must be integral and calculated. Therefore, we need to obtain suitable equations for calculating distribution functions on boundaries for a given boundary condition. The present study examined 2-D flow by a 2-D square lattice with nine velocities and temperature vectors (D2Q9 model) for modeling velocity of fluid-flow and temperature fields. The velocity and temperature vectors $c_0 \ldots c_8$, of the D2Q9 model are shown in fig. 2.

For each velocity and temperature vector, a particle DF is stored. The velocity of fluid-flow and temperature vectors of the D2Q9 model are presented in tab. 1.

Table 1. Velocity and temperature vectors of the D2Q9 model

i	0	1	2	3	4	5	6	7	8
c_i	$(0, 0)c$	$(1, 0)c$	$(0, 1)c$	$(-1, 0)c$	$(0, -1)c$	$(1, 1)c$	$(-1, 1)c$	$(-1, -1)c$	$(1, -1)c$

where $c = \Delta x/\Delta t$ and k is the Lattice velocity direction. The LBM used in the present work is the same as that employed in [38]. The DF are calculated by solving the Lattice Boltzmann equation (LBE), which is a special discretization of the kinetic Boltzmann equation. The two-phase Boltzmann's equation for a nanofluid can be expressed [39]:

$$f_i^\sigma(x+\mathrm{e}_i\Delta t, t+\Delta t) - f_i^\sigma(x,t) = -\frac{1}{\tau_f^\sigma}[f_i^\sigma(x,t) - f_i^{\sigma,\mathrm{eq}}(x,t)] + \left(\frac{2\tau_f^\sigma - 1}{2\tau_f^\sigma}\right)\left(\frac{F_i^\sigma \mathrm{e}_i \Delta t}{B_i c^2}\right) + \Delta t F_i \tag{2}$$

where $\sigma = 1, 2$ represent the base fluid and the nanoparticle components of the nanofluid and τ_f^σ is the relaxation time of component σ, respectively. Also, $B_i = 6$ for $i = 1\text{-}4$ and $B_i = 24$ for $i = 5\text{-}8$. Furthermore, in this equation e_i is the lattice velocity vector in the i^{th} direction and $f_i^{\sigma,\mathrm{eq}}$ is the particle equilibrium distribution function associated with motion along the i^{th} direction in the velocity space. The equilibrium density distribution functions of the σ^{th} component, $f_i^{\sigma,\mathrm{eq}}$ for the current 2-D application, based on D2Q9 model are:

$$f_i^{\sigma,\mathrm{eq}}(x,t) = \omega_i \rho^\sigma \left[1 + \frac{3\mathrm{e}_i u^{\sigma,\mathrm{eq}}}{c^2} + \frac{9(\mathrm{e}_i u^{\sigma,\mathrm{eq}})^2}{2c^4} - \frac{3(u^{\sigma,\mathrm{eq}})^2}{2c^2}\right] \tag{3}$$

The lattice space δx and the lattice time step δt are taken as unity and their ratio *is* $\delta x/\delta t$. The macroscopic density, kinematic viscosity, and velocity of the σ^{th} component are given by $\rho^\sigma(x,t) = \Sigma_i f_i^\sigma(x,t)$, $\nu^\sigma = (2\tau_f^\sigma - 1/6)c^2\Delta t$, and $u^\sigma = \Sigma_i f_i^\sigma(x,t)\mathrm{e}_i$, respectively. In this equation, the equilibrium velocities $u^{\sigma,\mathrm{eq}}$ is given by:

$$u^{\sigma,\mathrm{eq}} = \frac{1}{\rho^\sigma}\sum_i f_i^\sigma \mathrm{e}_i + \frac{F^\sigma \tau_f^\sigma \Delta t}{\rho^\sigma} \tag{4}$$

The corresponding equilibrium DF for fluid and solid, respectively, the LBE energy for nanofluid, based on D2Q9 model is defined:

$$g_i^\sigma(x+\mathrm{e}_i\Delta t, t+\Delta t) - g_i^\sigma(x,t) = \frac{1}{\tau_\theta^\sigma}[g_i^{\sigma,\mathrm{eq}}(x,t) - g_i^\sigma(x,t)] \tag{5}$$

The equilibrium energy distribution functions can be defined:

$$g_i^{\sigma,\mathrm{eq}} = \omega_i T^\sigma \left[1 + \frac{\mathrm{e}_i u^{\sigma,\mathrm{eq}}}{c^2} + \frac{9(\mathrm{e}_i u^{\sigma,\mathrm{eq}})^2}{2c^4} - \frac{3(u^{\sigma,\mathrm{eq}})^2}{2c^2}\right] \tag{6}$$

where g_i^σ is the i^{th} energy distribution function and τ_θ^σ is the thermal relaxation time and $T^\sigma = \Sigma_i g_i^\sigma$ is the temperature of the component σ. The corresponding thermal diffusivity is calculated as $\alpha^\sigma = (2\tau_f^\sigma - 1/6)\mathrm{c}^2\Delta t$.

The velocity and temperature vectors of the D2Q9 model are presented in tab. 2.

Table 2. Velocity and temperature vectors of the D2Q9 model

i	0	1	2	3	4	5	6	7	8
ω_i	4/9	1/9	1/9	1/9	1/9	1/36	1/36	1/36	1/36

The interaction forces between nanoparticles and base fluid considered in this method include the buoyancy force, the gravity force, the drag force, the Brownian diffusion force, and the thermophoresis force. The Boussinesq approximation is applied to exert buoyancy force. The buoyancy term is:

$$F_H = \rho g \beta \Delta T \tag{7}$$

where β is the thermal expansion coefficient and ΔT – the temperature difference. Thermophoresis force is written [40]:

$$F_\mathrm{T} = 3\pi\mu d_\mathrm{p}\left(2A\frac{k}{2k+k_\mathrm{p}}\frac{\mu}{\rho T}\right)\nabla T \tag{8}$$

where A is the coefficient and (k, μ, ρ) and (k_p) are thermophysical properties of nanofluid and particles, respectively. The drag force is obtained from Stokes law for small particles [40]:

$$F_\mathrm{D} = 3\pi\mu d_\mathrm{p}(V - V_P) \tag{9}$$

where V is the fluid speed and V_P – the nanoparticles speed.

Brownian motion is the random motion and the Brownian force can be expressed [40]:

$$F_\mathrm{B} = C\frac{k_b T}{R} \tag{10}$$

where C is the Brownian diffusion coefficient and is set to $1\cdot 10^{14}$, k_b – the Boltzmann constant, and R – the radius of nanoparticle. In this survey, we used CuO-nanoparticles. So, thermophysical nanofluid properties are assumed invariant, and are given in tab. 3.

Table 3. Thermophysical properties of water and CuO-nanoparticles

Material	ρ [kgm^{-3}]	C_P [Jkg^{-1}K^{-1}]	k [Wm^{-1}K^{-1}]	$\beta \cdot 10^5$ [k^{-1}]
Pure water	997.10	4179	0.61	21
CuO	6500	540	18	0.85

Validation for LBM

Figure 3 provides a complete comparison of the results of the present simulation with the previous results. The temperature and velocity profiles in the middle of enclosure are horizontal and gradually deviates towards the hot and cold walls. Figure 3 shows that our simulation results had acceptable accuracy and good agreement with Ahmed *et al.* [40] in Ra = 10^4 and Ra = 10^6.

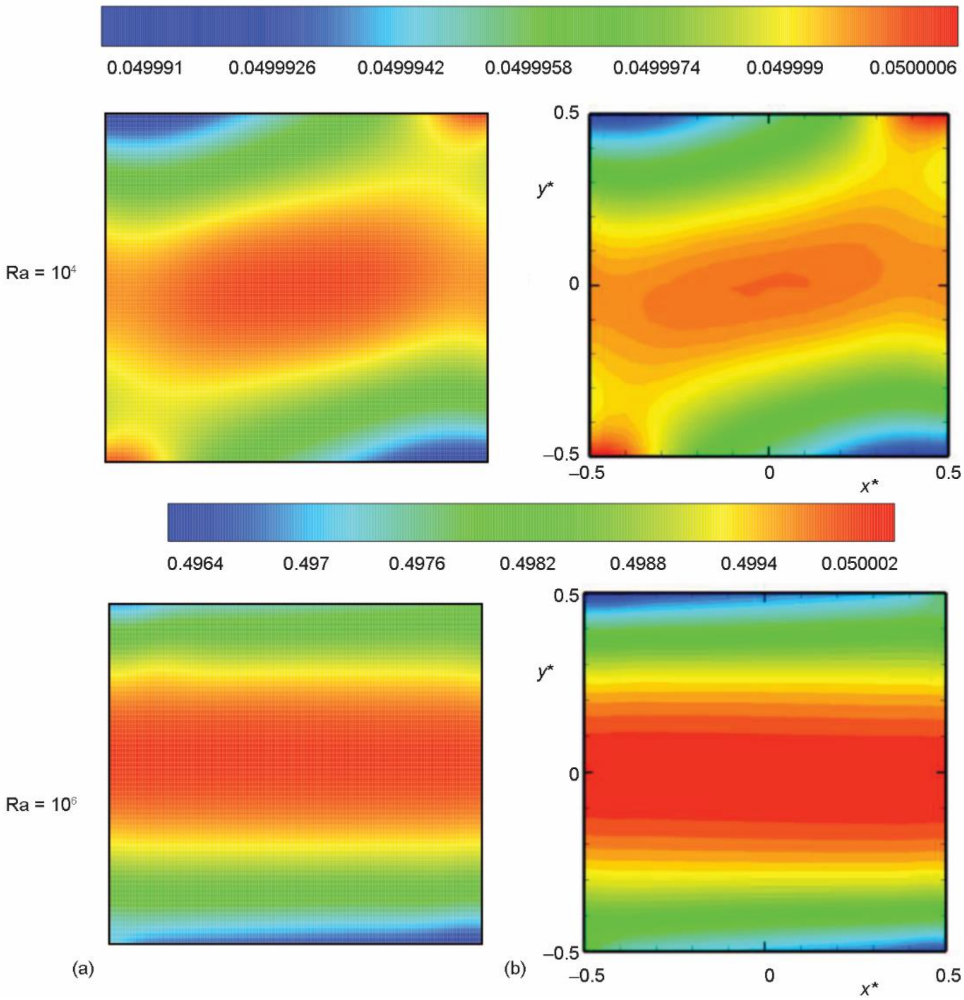

Figure 3. Nanoparticle volume fraction distribution at Ra = 10^6 in (a) present study, (b) [40]

Results and discussion

In present study, heat transfer rate of a two-phase CuO-water nanofluid under different heat flux in a cubical enclosure is investigated. The heat transfer characteristics are controlled by transfiguration of the enclosure in six case of different heat flux. Figure 4 shows comparison temperature fields between these cases under different heat flux. We selected cases that orientation of their temperate field were smooth and maximum less than 50 °C, $T_{\max} > 50$ °C. So, with these two conditions, we chose Cases 3 and 4 that Case 3 was better than Case 4, because Case 4 was suitable with $y/h > 0.7$. Also, the best selection is an enclosure with heat flux rate $3q''/2$ and heat flux array is triangular from down to up.

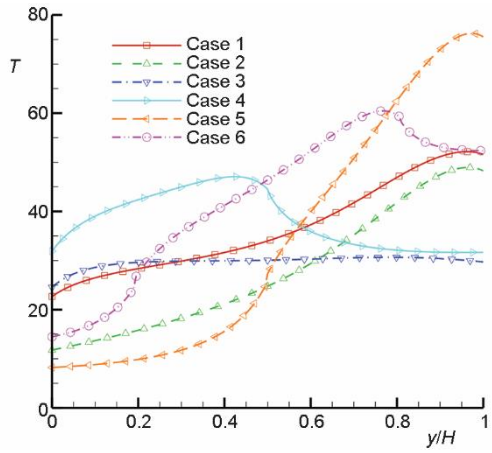

Figure 4. Comparison temperature fields between different enclosures under different heat flux

In fig. 5, streamlines, temperature fields and nanoparticle volume fraction with CuO-water nanofluid between Cases 3 and 4 are presented. This figure shows that gradations of streamlines, temperature fields and nanoparticle are smooth for Case 3. In Case 4, temperature fields are focused on below part of hot wall but in Case 3, temperature fields are all over the hot wall.

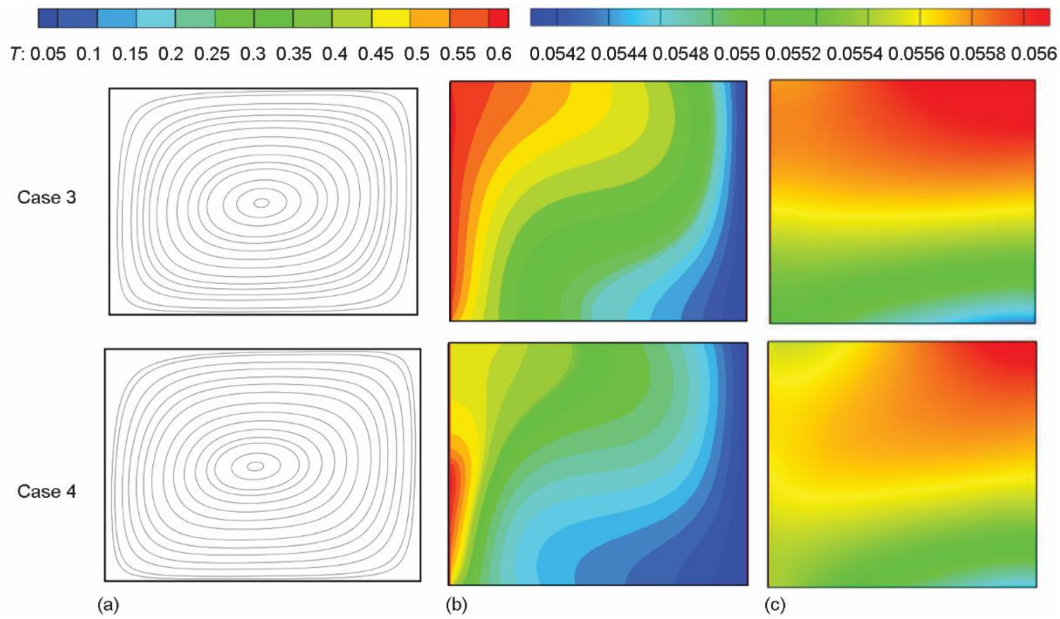

Figure 5. Comparison streamline (a), temperature fields (b), and nanoparticle volume fraction (c) between Cases 3 and 4

We designed solutions for Cases 1, 2, 5, and 6 to orientation of their temperate field become smooth and maximum less than 50 °C, $T_{\max} > 50$ °C. So, we simulated parallelogram enclosures with positive and negative angle in adiabatic walls. These approaches able to orientation of temperate field in enclosures become smooth. Figure 6 illustrates parallelogram enclosures with positive angle in Cases 1 and 2 cause to orientation of temperate field in these enclosures become smooth and $T_{\max} > 50$ °C. Also, parallelogram enclosures with negative angle in Case 6 with $y/H > 0.7$ gives smooth in orientation of temperate field with $T_{\max} > 50$ °C, but in Case 5, parallelogram enclosures with positive and negative angle were not suitable solutions.

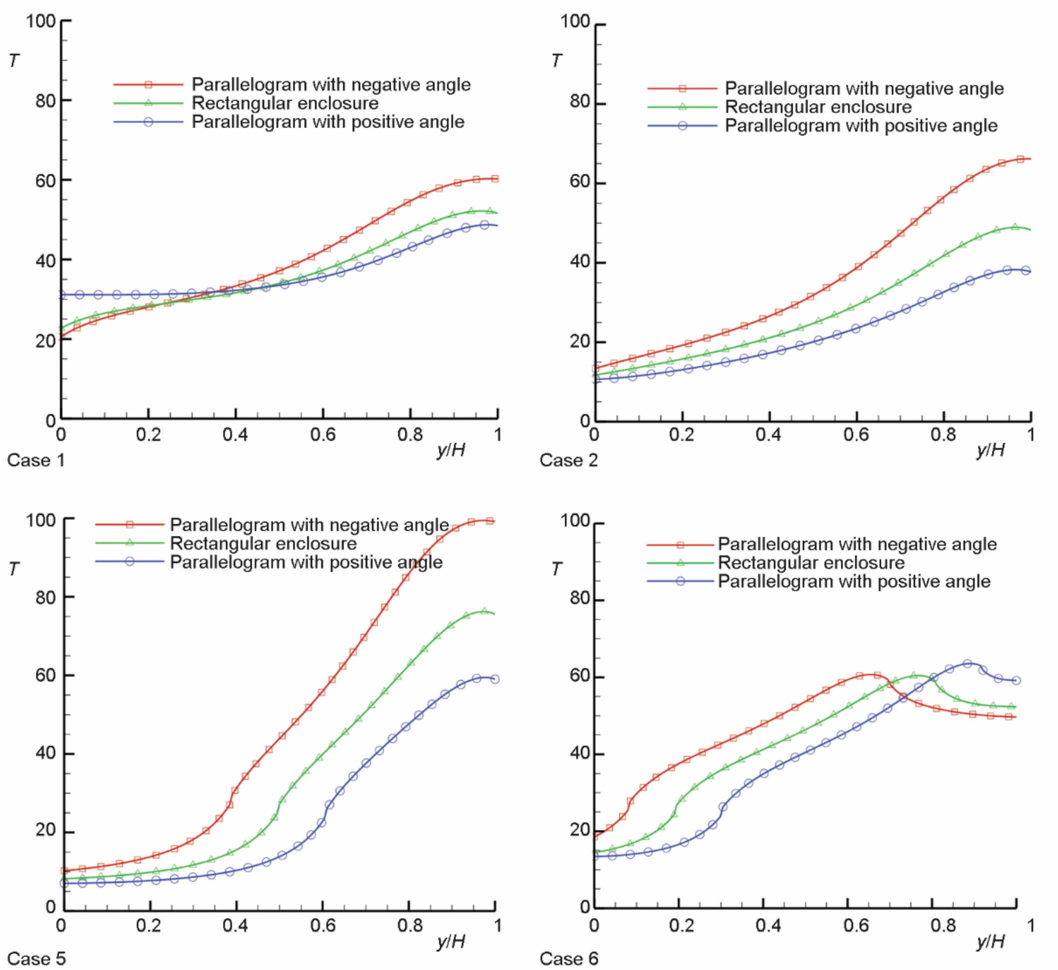

Figure 6. Comparison temperature fields between different enclosures under different heat flux

Figure 7 illustrated that in Cases 1 and 2 temperature fields under design parallelogram enclosure with positive angle were transferred better than normal conditions. Also, temperature fields in Case 6 with design parallelogram enclosure with negative angle had conclusions better than parallelogram enclosure with positive angle and normal conditions. These results agreed with fig. 6. Streamlines under conditions parallelogram enclosures with positive and negative angle were compacted and two-phase nanofluid-flow were intensity. According to fig. 8, all of these conditions are suitable for especial and different performances. For example, when we needed to compacted streamlines in cold wall so, parallelogram enclosure with negative angle in Case 1 was suitable.

In fig. 9 illustrated when we designed parallelogram enclosure with positive angle so, CuO-water nanoparticles volume fraction was transferred to cold wall more than normal conditions vice versa parallelogram enclosure with negative angle. So, we can better and faster transfer heat flux to cold wall in different situations.

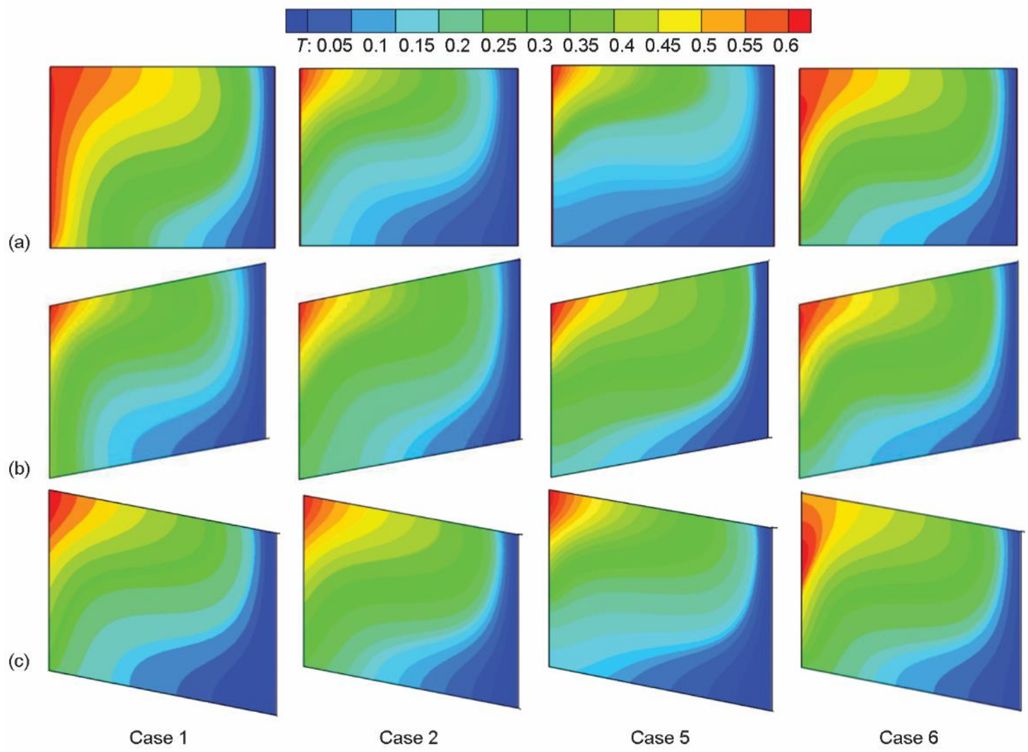

Figure 7. Comparison temperature fields between enclosures into (a) rectangular, (b) parallelogram with positive angle, and (c) parallelogram with negative angle

Table 4 presented average of temperature on the cold wall of enclosures. So, according to base of rectangular enclosures, variation rates of average of temperature in Cases 1 and 2, parallelogram enclosures with positive angle were 0.04% and –11%, respectively. Also in Case 6, parallelogram enclosure with negative angle had 0.01% increasing in rates of average of temperature. These compressions were done according to fig. 6 that we chose these improvement cases with conditions. Orientation of temperate field in these enclosures became smooth and $T_{\max} > 50$ °C. So, Case 1, parallelogram enclosures with positive angle and Cases 3 and 4 were best Cases that average of temperature in Case 1 was close to Case 4 with rectangular enclosure.

Table 4. Average of temperature on the left wall between different conditions of enclosures

Rectangular	Case 1	Case 2	Case 3	Case 4	Case 5	Case 6
Parallelogram with positive angle	36.532	27.804	29.760	38.228	34.148	42.305
Parallelogram with negative angle	37.900	24.741	–	–	29.577	43.483

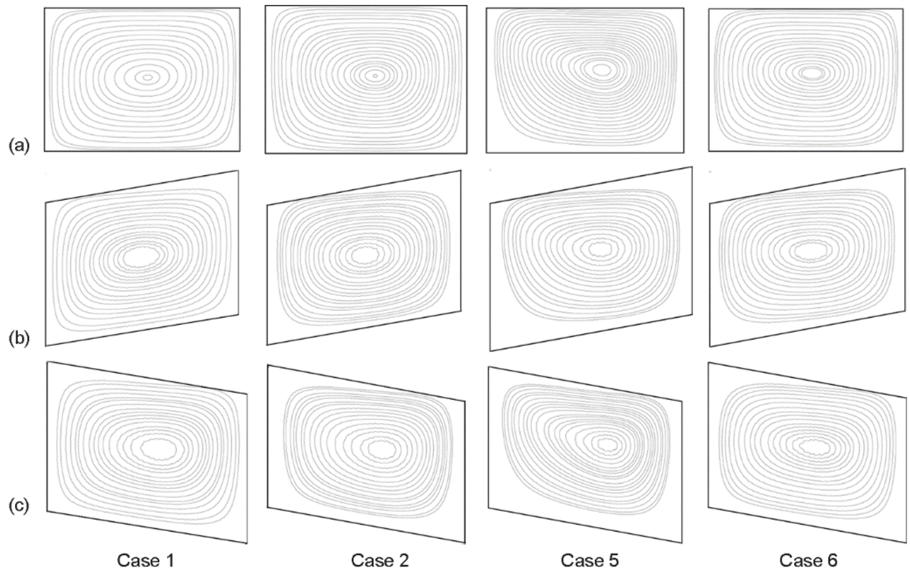

Figure 8. Comparison streamline between enclosures into (a) rectangular, (b) parallelogram with positive angle, and (c) parallelogram with negative angle

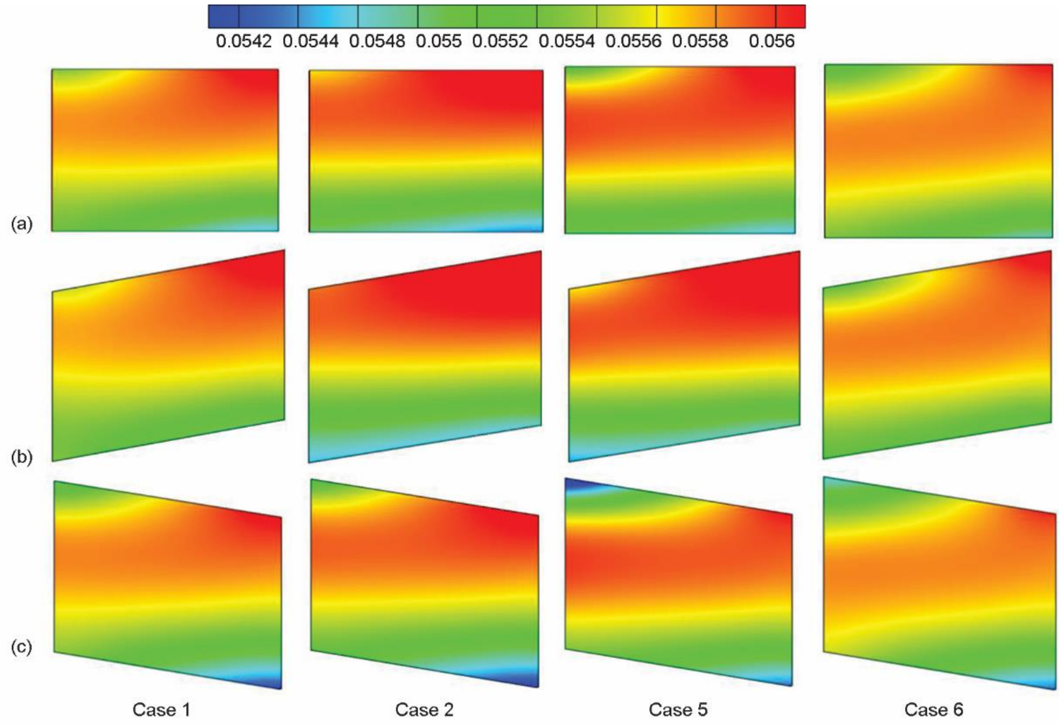

Figure 9. Comparison nanoparticle volume fraction between enclosures into (a) rectangular, (b) parallelogram with positive angle, and (c) parallelogram with negative angle

Conclusions

In this paper, a comprehensive numerical analysis and control the wall temperature fluctuations in a two-phase CuO-water nanofluid under different heat flux by designing the transfiguration of the enclosure was investigated. The D2Q9 LB method was used to solve the flow and temperature field. Streamlines, isotherms and nanoparticle volume fraction were exhibited for Cases 1-6. Also, we simulated rectangular and parallelogram enclosures with positive and negative angular adiabatic walls. Finally, the main results summarized:

- Investigations show that Cases 3 and 4 have approximately uniform temperature profiles on the hot wall and that their maximum temperature does not exceed 50 °C. Of course, given that Case 3 at all domain but Case 4 within range $y/H > 0.7$ exhibits quite acceptable behavior.
- The best choice is a rectangular enclosure with a triangular heat flux on the wall (maximum $3q''/2$).
- With increasing of cuo nanoparticles to the fluid at all of the enclosers, temperature field improved.
- Simulation of Cases 1, 2, 5, and 6 illustrated that the hot wall of Cases 1 and 2 with positive angle and Case 6 ($y/H > 0.7$) with negative angle have uniform temperature profiles with $T_{\max} < 50$ ºC.

Nomenclature

d_p – spherical particle diameter of the solid
f_i – particle density distribution function
f_i^{eq} – equilibrium particle density distribution function
g_i – particle energy distribution function
g_i^{eq} – equilibrium particle energy distribution function
k_b – Boltzmann constant
L – dimensions of channel, [m]
Ra – Rayleigh number, ($= g\beta\Delta TL^3/\nu\alpha$)
T_c – temperature of the cold wall, [K]
ΔT – temperature difference, [K]
x, y – coordinates, [m]

Greek Symbols

α – thermal diffusivity, [m^{2}s^{-1}]
β – thermal expansion, [K^{-1}]
ρ – density, [kgm^{-3}]
μ – dynamic viscosity, [kgm^{-1}s^{-1}]
ν – kinematic viscosity, [m^{2}s^{-1}]
τ_θ – relaxation time of temperature field
τ_f – relaxation time of flow field

Subscripts

c – cold
i – direction of lattice link
f – fluid

References

[1] Samarbakhsh, S., *et al.*, Experimental and Numerical Analysis of Eight Different Volutes with The Same Impeller in A Squirrel-Cage Fan, *Proceedings,* 2nd European Conference of Control and Mechanical Engineering, Milan, Italy, 2011, pp. 198-203

[2] Alinejad, J., *et al.*, Aerodynamic Optimization in The Rotor of Centrifugal Fan Using Combined Laser Doppler Anemometry and CFD Modeling, *World Applied Sciences Journal*, *17* (2012), 10, pp. 1316-1323

[3] Alinejad, J., *et al.*, Accretion of the Efficiency of a Forward-Curved Centrifugal Fan by Modification of the Rotor Geometry: Computational and Experimental Study, *International Journal of Fluid Mechanics Research*, *40* (2013), 6, pp. 469-481

[4] Esfahani, J. A., *et al.*, Lattice Boltzmann Simulation of Viscous-Fluid-flow and Conjugate Heat Transfer in A Rectangular Cavity with A Heated Moving Wall, *Thermophysics and Aeromechanics*, *20* (2013), 5, pp. 613-620

[5] Esfahani, J. A., *et al.*, Entropy Generation of Conjugate Natural Convection in Enclosures: The Lattice Boltzmann Method, *International Journal of Multiphase Flow, 27* (2013), 3, pp. 498-505

[6] Alinejad, J., *et al.*, Lattice Boltzmann Simulation of Forced Convection Over an Electronic Board with Multiple Obstacles, *Heat Transfer Research, 45* (2014), 3, pp. 241-262
[7] Alinejad, J., *et al.*, Numerical Stabilization of Three-Dimensional Turbulent Natural Convection Around Isothermal Cylinder, *Journal of Thermophysics and Heat Transfer, 30* (2016), 1, pp. 94-102
[8] Alinejad, J., *et al.*, Lattice Boltzmann Simulation of EGM and Solid Particle Trajectory Due to Conjugate Natural Convection, *Aerospace Science and Technology*, *4* (2016), 1, pp. 36-43
[9] Alinejad, J., *et al.*, Taguchi Optimization Approach for Three-Dimensional Nanofluid Natural Convection in a Transformable Enclosure, *Journal of Thermophysics and Heat Transfer*, *31* (2016), 1, pp. 1-7
[10] Alinejad, J., *et al.*, Taguchi Design of Three Dimensional Simulations for Optimization of Turbulent Mixed Convection in A Cavity, *Meccanica*, *52* (2017), 4-5, pp. 925-938
[11] Alinejad, J., *et al.*, Optimization of 3-D Natural Convection Around the Isothermal Cylinder Using Taguchi Method, *Journal of Applied Mechanics and Technical Physics*, *57* (2016), 1, pp. 117-126
[12] Fallah, K., *et al.*, The Influence of Micro Air Jets On Mixing Augmentation of Fuel in Cavity Flameholder at Supersonic Flow, *Aerospace Science and Technology*, *76* (2018), 1, pp. 187-193
[13] Peiravi, M. M., *et al.*, Numerical Study of Fins Arrangement and Nanofluids Effects On Three-Dimensional Natural Convection in The Cubical Enclosure, *Transp. Phenom. Nano Micro Scales*, *7* (2019), 2, pp. 97-112
[14] Peiravi, M. M., *et al.*, Hybrid Conduction, Convection and Radiation Heat Transfer Simulation in a Channel with Rectangular Cylinder, *Journal of Thermal Analysis and Calorimetry*, *140* (2020), Nov., pp. 2733-2747
[15] Peiravi, M. M., *et al.*, 3-D Optimization of Baffle Arrangement in A Multi-Phase Nanofluid Natural Convection Based On Numerical Simulation, *International Journal of Numerical Methods for Heat and Fluid-flow*, *30* (2019), 5, pp. 2583-2605
[16] Liang, G., *et al.*, Two-Phase Heat Transfer of Multi-Droplet Impact On Liquid Film, *International Journal of Heat and Mass Transfer*, *139* (2019), 1, pp. 832-847
[17] Boubaker, R., *et al.*, Effect of Self-Rewetting Fluids on the Liquid/Vapor Phase Change in a Porous Media of Two-Phase Heat Transfer Devices, *International Journal of Heat and Mass Transfer*, *136* (2019), 1, pp. 655-663
[18] Park, Y., *et al.*, Heat Transfer Augmentation in Two-Phase Flow Heat Exchanger Using Porous Microstructures and A Hydrophobic Coating, *Applied Thermal Engineering*, *153* (2019), 1, pp. 433-447
[19] Burk, B. E., *et al.*, Computational Examination of Two-Phase Microchannel Heat Transfer Correlations with Conjugate Heat Spreading, *International Journal of Heat and Mass Transfer, 132* (2019), 1, pp. 68-79
[20] Zhang, K., *et al.*, Experimental Investigations On Single-Phase Convection and Two-Phase Flow Boiling Heat Transfer in an Inclined Rod Bundle, *Applied Thermal Engineering, 148* (2019), 1, pp. 340-351
[21] Liu, Y., *et al.*, Uncertainty Quantification of Two-Phase Flow and Boiling Heat Transfer Simulations Through a Data-Driven Modular Bayesian Approach, *International Journal of Heat and Mass Transfer, 138* (2019), 1, pp. 1096-1116
[22] Jiang, G., *et al.*, Flow and Heat Transfer Characteristics of Mist/Steam Two-Phase Flow in The U-Shaped Cooling Passage with 60 Deg. Ribs, *International Communications in Heat and Mass Transfer, 105* (2019), 1, pp. 73-83
[23] Song, Q., *et al.*, R14 Flow Condensation Heat Transfer Performance: Measurements and Modeling Based On Two-Phase Flow Patterns, *International Journal of Heat and Mass Transfer, 136* (2019), 1, pp. 298-311
[24] Lee, J., *et al.*, Experimental and Computational Investigation On Two-Phase Flow and Heat Transfer of Highly Subcooled Flow Boiling in Vertical Upflow, *International Journal of Heat and Mass Transfer, 136* (2019), 1, pp. 1199-1216
[25] Zhang, X., *et al.*, Two-Phase Flow and Heat Transfer in A Self-Developed MRI Compatible LN2 Cryoprobe and its Experimental Evaluation, *International Journal of Heat and Mass Transfer, 136* (2019), 2, pp. 709-718
[26] Moezzi, M., *et al.*, Hysteretic Heat Transfer Study of Liquid-Liquid Two-Phase Flow in A T-Junction Microchannel, *International Journal of Heat and Fluid-flow, 77* (2019), 1, pp. 366-376
[27] Alinejad, J., *et al.*, Numerical Analysis of Secondary Droplets Characteristics Due to Drop Impacting on 3-D Cylinders Considering Dynamic Contact Angle, *Meccanica*, *55* (2020), 10, pp. 1975-2002
[28] Domairry, G. D., *et al.*, Evaluation of The Heat Transfer Rate Increases in Retention Pools Nuclear Waste, *International Journal of Nano Dimension*, *6* (2015), 4, pp. 385-398

[29] Domairry, G. D., *et al.*, Evaluation of the Heat Transfer Rate Increases in Retention Pools Nuclear Waste, *International Journal of Nano Dimension*, *6* (2015), 4, pp. 385-398

[30] Peiravi, M. M., *et al.*, Survey of Nano-Bio Convection Flow in a Horizontal Channel by Using AGM and FlexPDE Software, *Proceedings,* 3rd Conference of Heat and Mass Transfer, Nov. 22, Amol, Iran, 2017

[31] Peiravi, M. M., *et al.*, Survey and Analysis of the Thermal Flux of a Nanofluid Droplet with a Variable Conductive Coefficient in the Cooling of Nuclear Reactors, *Proceedings,* 1st International Conference on Modern Technologies in Science, Amol, Iran, 2017

[32] Domairry, G. D., *et al.*, Survey on Increasing the Heat Transfer Rate in Spent Fuel (Nuclear Wastes) Pool with Free Convection Boundary Layer Flow on a Vertical Cone in a Porous Medium for Newtonian Nanofluid with Application of Homotopy Analysis Method (HAM), *Proceedings,* 8th international Conference on New Advances in Engineering Sciences, Amol, Iran, 2014

[33] Peiravi, M. M., *et al.*, Analysis of Non-Newtonian Nanofluid Natural Convection Flow, Sodium Alginate (SA) between Two Vertical Flat Plates, Publication Description, *Proceedings,* 17th Fluid Dynamics Conference, Shahrood, Iran, 2017

[34] Asadi, Z., *et al.*, Survey of Nano-Bio Convection Flow in a Horizontal Channel by Using AGM and FlexPDE Software, *Proceedings,* 3rd Conference of Heat and Mass Transfer, Amol, Iran, 2017

[35] Asadi, Z., *et al.*, Survey and Analysis of the Thermal Flux of a Nanofluid Droplet with a Variable Conductive Coefficient in the Cooling of Nuclear Reactors, *Proceedings,* 1st International Conference on Modern Technologies in Science, Amol, Iran, 2017

[36] Domairry, G. D., *et al.*, Survey On Increasing the Heat Transfer Rate in Spent Fuel (Nuclear Wastes) Pool with Free Convection Boundary Layer Flow on a Vertical Cone in a Porous Medium for Newtonian Nanofluid with Application of Homotopy Analysis Method (HAM), *Proceedings,* 8th international Conference on New Advances in Engineering Sciences, Amol, Iran, 2014

[37] Aliyari, f., *et al.*, Analysis of Non-Newtonian Nanofluid Natural Convection Flow, Sodium Alginate (SA) between Two Vertical Flat Plates, *Proceedings,* 17th Fluid Dynamics Conference, Shahrood, Iran, 2017

[38] Mezrhab, A., *et al.*, Lattice Boltzmann Modeling of Natural Convection in an Inclined Square Enclosure with Partitions Attached to Its Cold Wall, *International Journal of Heat and Fluid-flow, 27* (2006), 3, pp. 456-465

[39] Xuan, Y., *et al.*, Lattice Boltzmann Model for Nanofluids, *Heat and Mass Transfer, 41* (2005), 3, pp. 199-205

[40] Ahmed, M., *et al.*, Natural Convection in a Differentially-Heated Square Enclosure filled with a Nanofluid: Significance of the Thermophoresis Force and Slip/Drift Velocity, *International Communications in Heat and Mass Transfer, 58* (2014), 4, pp. 1-11

Paper submitted: May 24, 2020
Paper revised: October 27, 2020
Paper accepted: October 29, 2020